Materials Science & Engineering A 806 (2021) 140832

Contents lists available at ScienceDirect

Materials Science & Engineering A

journal homepage: http://www.elsevier.com/locate/msea

An examination of microstructural evolution and homogeneity in a magnesium AZ80 alloy processed by high-pressure torsion

Nian Xian Zhang [a,b], Megumi Kawasaki [c], Hua Ding [a,**], Terence G. Langdon [d,e,*]

[a] School of Materials Science and Engineering, Northeastern University, Shenyang, Liaoning, 110819, PR China
[b] Materials Department, Crown Technology, Downsview Road, Wantage, OX12 9BP, UK
[c] School of Mechanical, Industrial and Manufacturing Engineering, Oregon State University, Corvallis, OR, 97331, USA
[d] Materials Research Group, Department of Mechanical Engineering, University of Southampton, Southampton, SO17 1BJ, UK
[e] Departments of Aerospace & Mechanical Engineering and Materials Science, University of Southern California, Los Angeles, CA, 90089-1453, USA

ARTICLE INFO

Keywords:
Hardness
High-pressure torsion
Homogeneity
Magnesium alloy
Shear instabilities

ABSTRACT

A magnesium AZ80 alloy with an initial grain size of ~250 μm was processed by high-pressure torsion for up to 12 turns at room temperature. The processing produced increased hardness and significant grain refinement with average grain sizes of ~320 and ~200 nm at the edges of the discs after 1 and 12 turns, respectively. Microstructural examinations on different planes along the thickness direction of the discs revealed the presence of shear bands and twin boundaries and there were significant inhomogeneities even after 12 turns. The results show the presence of well-defined vortices having similarities to the well-established Kelvin-Helmholtz shear instabilities in fluid flow.

1. Introduction

The processing of bulk solids through the application of severe plastic deformation (SPD) has received much attention over the last decade because of the potential for achieving grain refinement to the submicrometer or even the nanometer range [1]. In SPD processing, a solid is subjected to a high strain without incurring any significant change in the overall dimensions of the sample. Several different SPD techniques are now available but most attention has focused on the two procedures of equal-channel angular pressing (ECAP) and high-pressure torsion (HPT) [2]. In ECAP a bar or rod is pressed through a die constrained within a channel that is bent through a sharp angle [3] and in HPT the sample, generally in the form of a thin disc, is held between massive anvils, subjected to a high applied pressure and then concurrent torsional straining [4]. In practice, processing by HPT is especially attractive because it leads to grain sizes that are generally smaller than those produced by ECAP [5,6] and also it produces samples having higher fractions of high-angle grain boundaries [7].

Calculations show that the strain introduced in HPT processing is not constant and instead it varies from zero at the centre of the disc to a maximum value at the periphery [8]. This suggests, therefore, that the microstructures developed in HPT will be inhomogeneous and there have been several investigations directed specifically to evaluating the level of homogeneity in materials processed by HPT. In an early study using an austenitic steel it was shown that at low numbers of HPT turns the deformation, as determined from microhardness measurements, was high at the edge of the disc but low and close to zero at the centre [9]. However, the deformation became more equilibrated across the sample with increasing numbers of turns although there remained a small central region that was essentially undeformed even after 16 turns [9]. In a later investigation using high-purity aluminum the hardness was measured on different planes of sectioning through the HPT discs and the results showed that the hardness was almost constant across the disc after 5 turns and after 20 turns the hardness was fully homogeneous throughout the sample [10]. This gradual evolution towards a reasonable level of homogeneity is consistent with the theoretical predictions based on strain gradient plasticity modeling [11].

Nevertheless, later studies using an AZ31 magnesium alloy showed persistent evidence for heterogeneity in HPT samples after 5 turns [12] and, by taking observations on through-thickness planes by sectioning vertically, there were consistent higher hardness values near the bottoms of the discs [13]. There are also other reports showing high levels of microstructural inhomogeneity in AZ31 and AZ91 magnesium alloys [14,15] and texture heterogeneities in a ZK60 magnesium alloy [16]

* Corresponding author. Materials Research Group, Department of Mechanical Engineering, University of Southampton, Southampton, SO17 1BJ, UK.
** Corresponding author.
E-mail addresses: dingh@smm.neu.edu.cn (H. Ding), langdon@soton.ac.uk (T.G. Langdon).

https://doi.org/10.1016/j.msea.2021.140832
Received 12 September 2020; Received in revised form 6 January 2021; Accepted 22 January 2021
Available online 27 January 2021

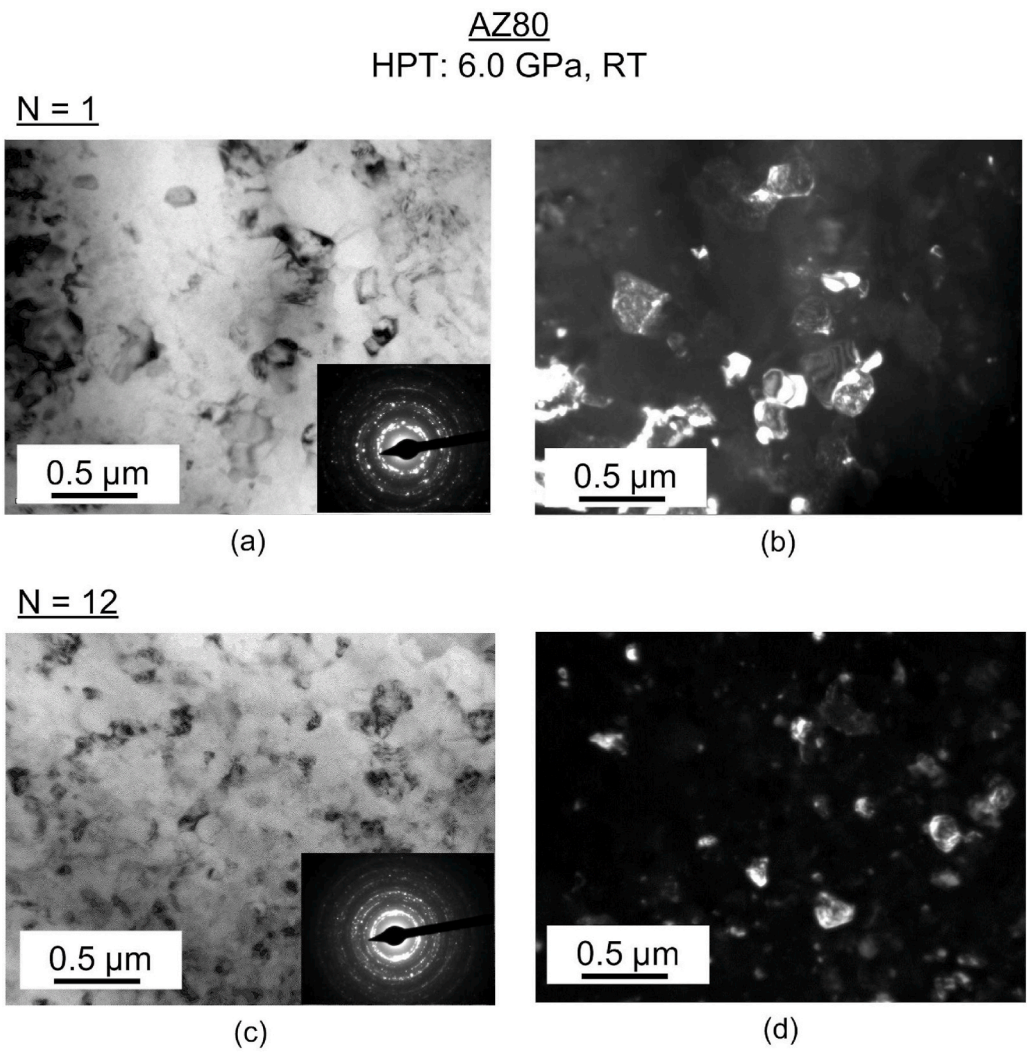

Fig. 1. TEM micrographs and SAED patterns on left and the corresponding dark field images on right at the edge regions of discs after HPT under 6.0 GPa through (a, b) 1 turn and (c,d) 12 turns.

after processing up to 5 revolutions. These results suggest, therefore, that there may be a difference between the developments of hardness homogeneity in face-centred cubic (f.c.c.) and hexagonal close-packed (h.c.p.) metals when processing by HPT. A comprehensive review of the hardness variations in different materials when testing by HPT is available elsewhere [17].

The present research was initiated in order to investigate the evolution of homogeneity on the cross-sectional planes of a magnesium AZ80 alloy. This material was selected as a representative magnesium alloy for use in this investigation because information is already available describing the mechanical properties of the alloy [18,19] and there are also a large number of reports describing the SPD processing of this alloy using either ECAP [20–29] or HPT [30–32].

2. Experimental material and procedures

The experimental material used in this investigation was a magnesium AZ80 alloy containing, in wt.%, 8.50 Al, 0.50 Zn, 0.10 Mn, 0.10 Si, 0.05 Cu, 0.005 Fe and 0.005 Ni. The as-cast material was solution annealed at 673 K for 24 h and then forged with a deformation ratio of ~50%. A description of the microstructure of the alloy under forged conditions was given in an earlier study [21]. The forged ingot was cut into rods with diameters of 10.0 mm and discs were cut from the rods with thicknesses of ~1.0 mm and then polished to final thicknesses of ~0.83 mm. In the forged condition, the average grain size was ~250 μm and the average Vickers microhardness, Hv, was about 60. The processing by HPT was conducted under an applied pressure, *P*, of 6.0 GPa at room temperature using a facility operating under quasi-constrained conditions [33,34] at a rotational speed of 1 rpm. The discs were processed by HPT for total numbers, *N*, of 1/2, 1 and 12 turns.

After processing, the discs were mounted in resin, ground with abrasive papers, polished with diamond paste and then polished using a colloidal silica solution. The polished surfaces were etched with an acetic-picral solution to reveal the grain boundaries and the microstructures were recorded using an optical microscope. Following microstructural examination, all discs were mounted and polished to a mirror-like surface and these surfaces were used to record the values of the Vickers microhardness. The hardness measurements were taken

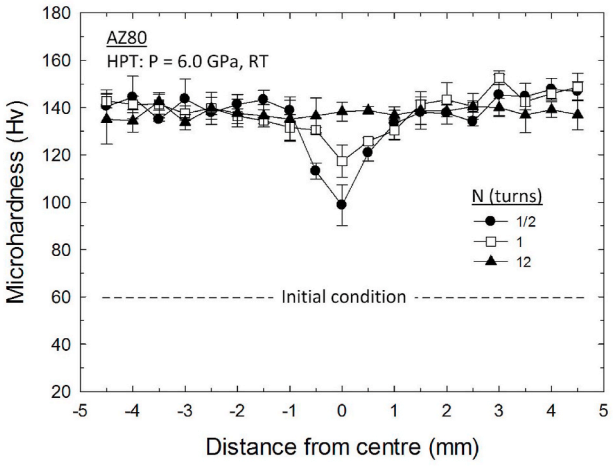

Fig. 2. Vickers microhardness versus distance from the centre of AZ80 discs tested under an applied pressure of 6.0 GPa through 1/2, 1 and 12 turns: the lower dashed line denotes the initial hardness without HPT.

using a Vickers indenter operating under a load of 200 gf with a dwell time of 15 s. The average values of Hv were recorded on each disc by taking measurements at selected positions along disc diameters with the individual points separated by incremental distances of 0.75 mm. The microhardness values were measured along a central line on a cross-section of each disc and for each point the average value was determined from four separate measurements taken at points arranged uniformly around the selected position and separated from this position by distances of 0.375 mm.

The microstructures were examined by transmission electron microscopy (TEM) using a Cs-corrected JEOL JEM-2100 F with an accelerating voltage of 20 kV. Samples were prepared by punching discs of 3.0 mm in diameter from the centre and edge of each HPT sample and all TEM discs were taken from the middle sectional planes in the thickness directions of each HPT disc. The TEM discs were thinned using mechanical polishing and a Gatan Precision Ion Polishing System (PIPS) operating at 4 kV with an angle of 2–8°. Selected area electron diffraction (SAED) patterns were recorded using an aperture having a diameter of 12.3 μm.

3. Experimental results

3.1. Grain size and hardness after processing by HPT

In Fig. 1, representative TEM images are shown on the left and the corresponding dark field images on the right for the edge regions of the discs after (a,b) 1 turn and (c,d) 12 turns together with the corresponding SAED patterns. The grain size was measured using dark field images because the individual grains are then more visible than in the bright field images. More than 100 grains were measured for each sample condition. The average grain sizes were determined at the disc edges as ~320 and ~200 nm after 1 and 12 turns, respectively. It is readily evident from the SAED patterns that a large fraction of these ultrafine grains are separated by boundaries having high angles of misorientation.

The variation in the Vickers microhardness across the diameter of each disc is shown in Fig. 2 where the lower dashed line denotes the initial solution annealed and forged condition with Hv ≈ 60 and the scatter on the individual measurements around each point was used to determine the 95% error bars. The results show that the hardness is low in the central region over a diameter of ~3 mm after 1/2 turn but the hardness values in the central region increase with further straining and all hardness values across the diameter are reasonably similar after 12 turns. This behaviour is similar to that reported in several other metals when processing by HPT [35–38].

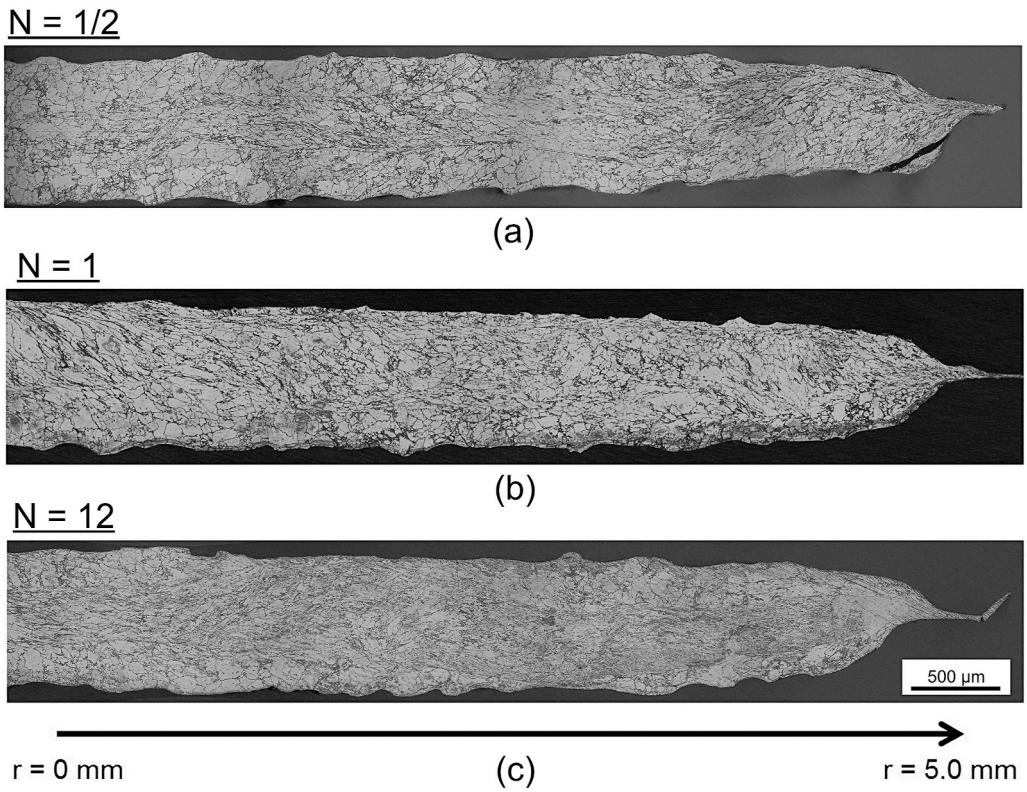

Fig. 3. Flow patterns in the cross-sectional planes of HPT samples after processing through (a) 1/2, (b) 1 and 12 turns: the lower arrow denotes a half radius.

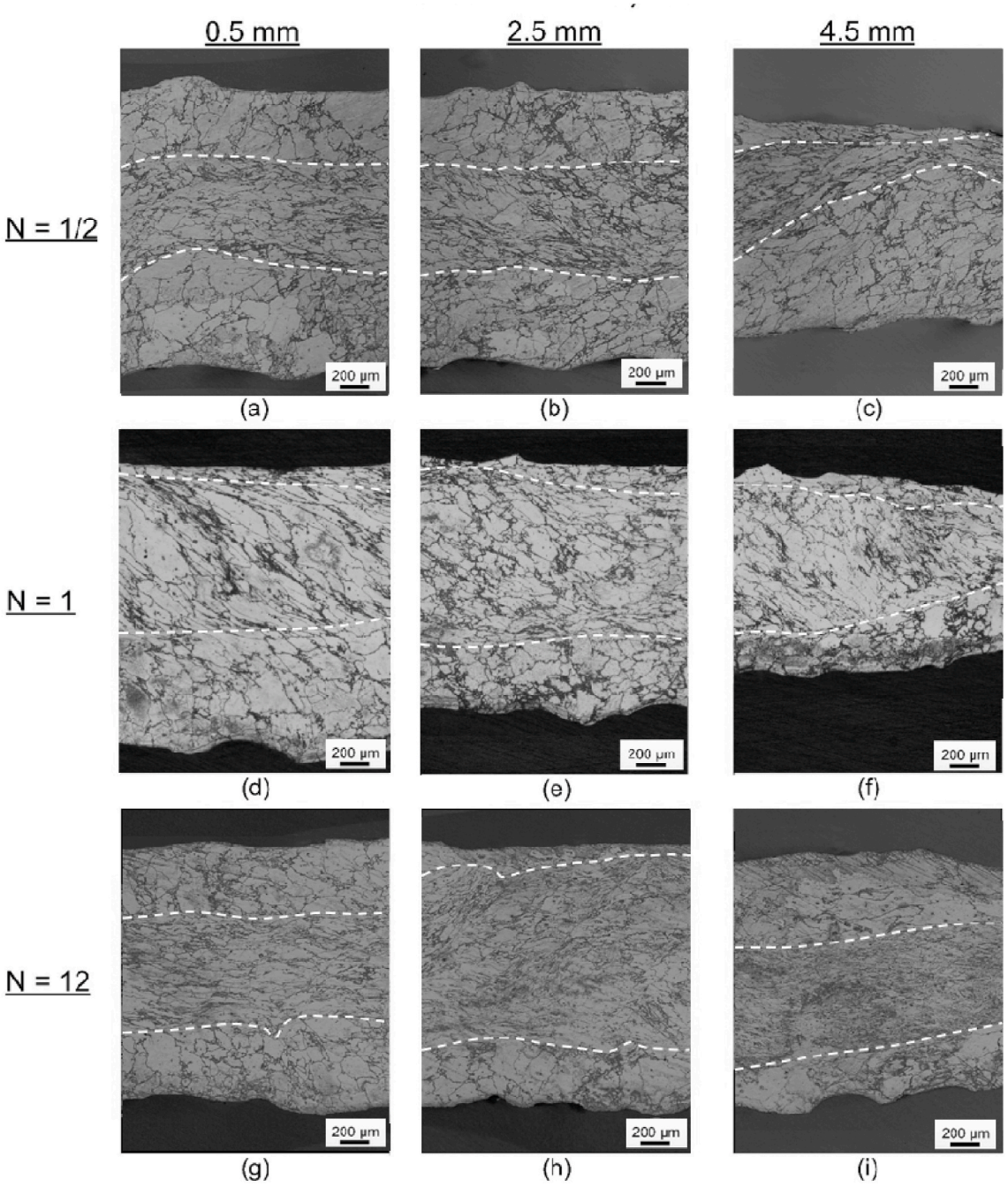

Fig. 4. Optical images at different radial positions from the centres of the discs after HPT through (a–c) 1/2, (d–f) 1 and (g–i) 12 turns.

3.2. The nature of inhomogeneity after HPT processing

Fig. 3 shows cross-sectional planes obtained by cutting the discs vertically after 1/2, 1 and 12 turns with the lower arrow denoting a half radius on the disc. Inspection shows there are deformed areas with visible well-defined flow patterns and also areas in each disc without any clear flow pattern although in practice the separation between these areas is not easily discernible in Fig. 3. To provide a better representation, more detailed images at higher magnifications are shown in Fig. 4 where the extent of deformation is equal to (a,b,c) 1/2, (d,e,f) 1 and (g,h, i) 12 turns, respectively, and the three columns were taken at radial positions on the discs corresponding to distances of 0.5, 2.5 and 4.5 mm from the centres of the discs, respectively. Close inspection shows the presence of shear bands in some of these samples and this matches earlier observations on an AZ91 magnesium alloy [15].

All of these images were recorded at the same high magnification and the areas with different flow patterns are denoted by the broken lines where well-defined flow occurs in the central cross-sectional region of each disc between the broken lines. Thus, in Fig. 3(a) near the centre of the disc there is a relatively narrow area with a distinct flow pattern in the middle plane whereas the remainder of the disc has limited flow after HPT. The areas with well-delineated flow are defined in Fig. 4 using the broken lines and it is apparent that these areas tend to widen with increasing numbers of turns and they tend to be widest at the mid-radius positions rather than at either the centre or the outer edge of each disc. Thus, well-defined flow occurs in the vicinity of radial positions of at least 2.5 mm rather than at the outer edge of each disc. This effect is demonstrated by considering the areas within the dashed lines in Fig. 4 (b,e and h).

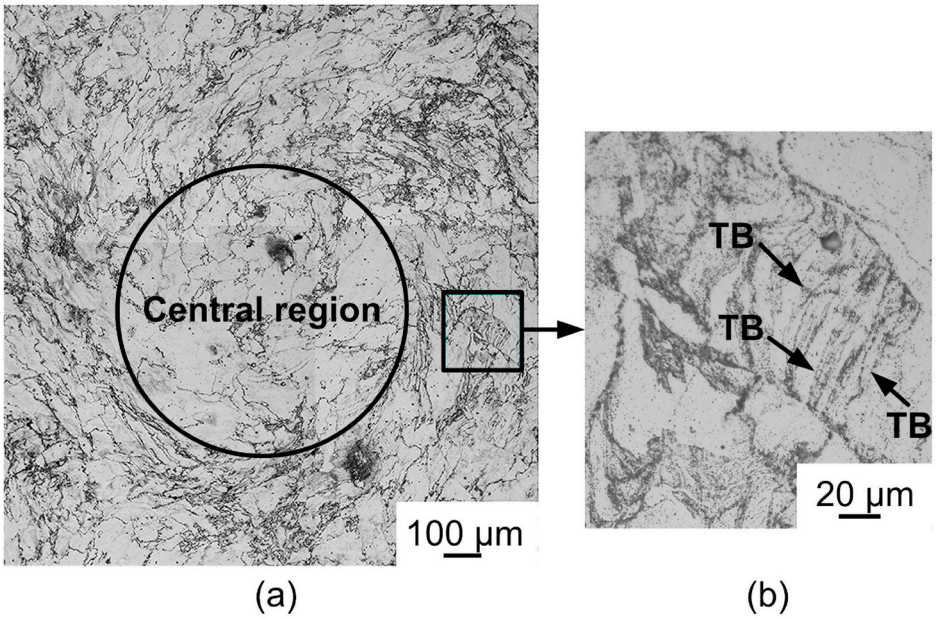

Fig. 5. Optical montage showing (a) a wide area around the central region of a disc and (b) a magnified image of the rectangular area marked in (a) after processing by HPT at 6.0 GPa for 1 turn: TB denotes twin boundaries.

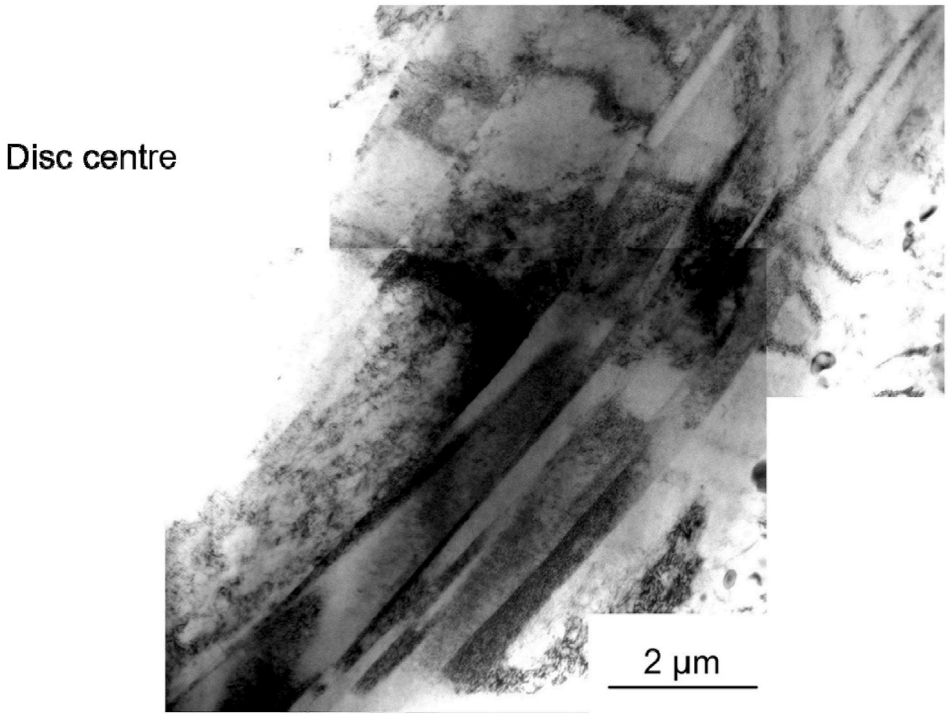

Fig. 6. A TEM image in the central region after processing by HPT at 6.0 GPa for 1 turn: the disc centre is located at the upper left corner of the image.

3.3. The nature of deformation in the central region of the disc after processing by HPT

The strain introduced in HPT processing is given by the expression $2\pi Nr/h\sqrt{3}$, where r is the radial distance from the centre of the disc and h is the initial height (or thickness) of the disc [8]. It follows from this expression that the strain is zero in the centre of the disc where $r = 0$ but nevertheless many results show an evolution towards a general homogeneity in hardness across the discs with increasing numbers of HPT turns [39,40]. In some materials, a homogeneity in hardness may be achieved only after the imposition of a very high strain through processing by a large number of HPT turns. For example, in a sandwich-like structure in which three discs were processed by HPT at 6.0 GPa by stacking the discs in the sequence of Al/Mg/Al, a hardness homogeneity was not visible across the disc diameter after 60 turns but it was attained after processing through 100 turns [41,42].

In order to more fully investigate the deformation occurring in the central region of the HPT discs, Fig. 5(a) shows an example of the disc centre after processing through 1 turn. Close inspection shows there are separate regions having different shear patterns with a central core

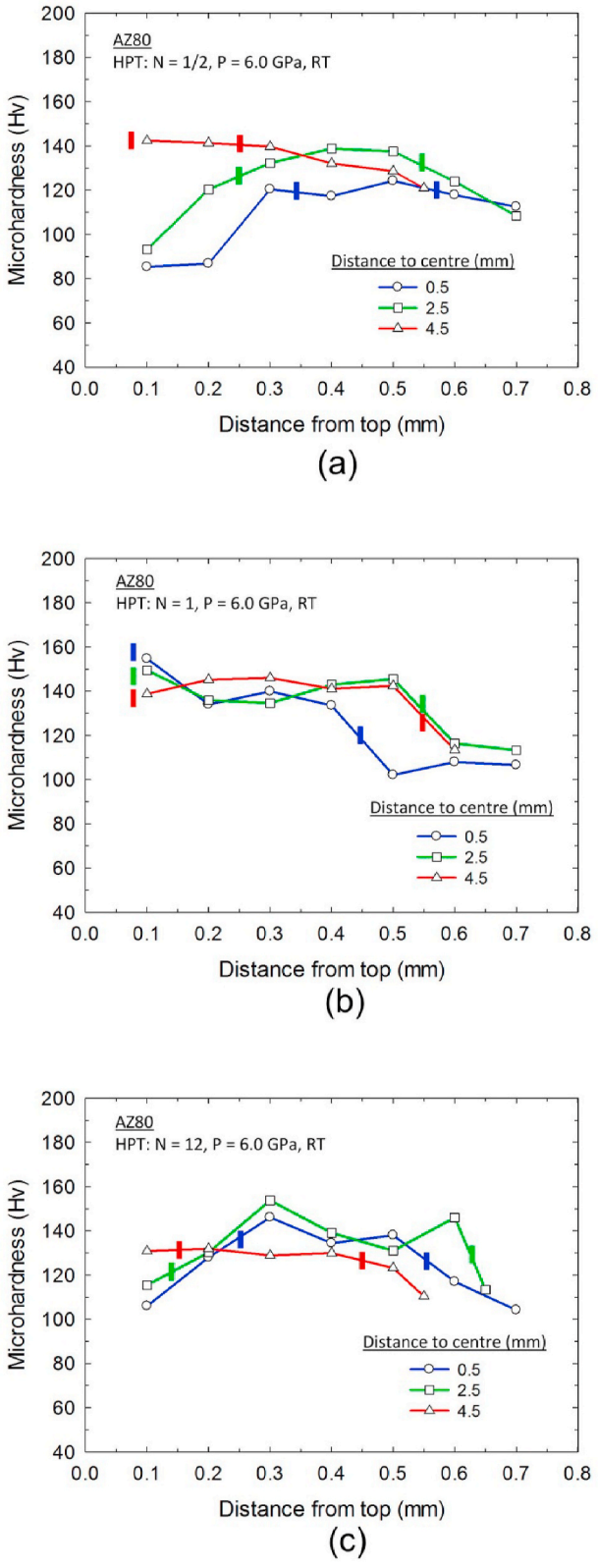

Fig. 7. The measured microhardness values at various radial positions as a function of distance from the top surfaces of the discs for HPT samples processed through (a) 1/2, (b) 1 and (c) 12 turns.

region which is reasonably well-defined and an outer region where there is a flow pattern.

Thus, around the central core there is a whirlpool-like flow showing only limited deformation where the substructure maintains a reasonably equiaxed shape. This central region is consistent with, and generally matches, the lower values of hardness recorded at the centre of the disc as shown in Fig. 2 and the overall appearance of this central region is similar to reports for other materials as, for example, a Cu-5% Al alloy where the measured hardness at the centre after 1 turn was exceptionally low [43]. In addition, the presence of local swirls and vortices is similar to several reports on the HPT processing of stainless steel [44–47] and a Cu–Ag alloy [48]. Outside of this central region, close inspection reveals the presence of many twin boundaries (TB) and examples are shown in Fig. 5(b) which is a higher magnification image of the small square indicated on the right side of Fig. 5(a). This microstructure involves deformation twinning [49,50] and is clearly evident in the TEM image shown in Fig. 6 which was taken from the same disc after 1 turn within an area similar in position to the region presented in Fig. 5(b).

3.4. The measured hardness values at through-thickness positions after HPT processing

Hardness values were measured at positions of ~0.5, ~2.5 and ~4.5 mm from the centre of each disc on vertically cut sections along the through-thickness directions at every 0.1 mm from the top to the bottom surface. These results are presented in Fig. 7 after (a) 1/2, (b) 1 and (c) 12 turns, respectively. It should be noted that the measurement points located between the 2 bars on each curve represent results recorded within areas where there were clear flow patterns as designated in Fig. 4 and in these areas the recorded microhardness values tend to be slightly higher than those recorded from areas without clear flow patterns.

In order to evaluate the extent of homogeneity within the HPT disc processed through the maximum of 12 turns, careful thinning was conducted to examine the disc at different positions corresponding to cross-sectional planes lying parallel to the upper and lower surfaces of the disc and displaced from the lower surface by distances of 0.40, 0.55 and 0.65 mm, respectively. This procedure is illustrated schematically on the left in Fig. 8 and relevant micrographs were recorded over broad areas, having widths of ~0.7 mm, from the centre to the edge of the disc. These individual micrographs were then assembled to provide a broad montage of each area from the centre to the edge as illustrated on the right in Fig. 8 corresponding to heights from the lower surface of (a) 0.65, (b) 0.55 and (c) 0.40 mm, respectively. Inspection of these images again reveals the occurrence of different shear morphologies with areas of high deformation involving intense and complex flow patterns contained within the rectangular boxes marked in Fig. 8(a–c). Although these areas of high deformation are generally not well-defined at this magnification, it is reasonable to conclude that deformation is highly concentrated over areas corresponding to sectional lengths that are approximately equivalent to the lengths of the rectangular boxes of ~1.2 mm in Fig. 8(a), ~3.7 mm in Fig. 8(b) and ~4.6 mm in Fig. 8(c). Therefore, the extent of these areas of high deformation gradually increases with increasing displacement towards the mid-plane in the HPT disc.

In addition, it is important to note that Figs. 3(c) and Fig. 4(g, h and i) are in excellent agreement with Fig. 8 where the heavily deformed area is located at the middle plane on the cross-section and it is narrow at the centre and edge of the disc but wide at the mid-radius position. From the perspective of Fig. 8, it is apparent for the disk after 12 HPT turns that if the disc is thinned from the upper surface towards the middle plane then the heavily deformed area is gradually revealed starting from the mid-radius position in Fig. 8(a) and gradually extending to cover almost the whole disc when thinned to the middle plane within the disc in Fig. 8 (c). Moreover, this widely extended microstructure with severe straining at the mid-plane position leads to a reasonably homogenous hardness

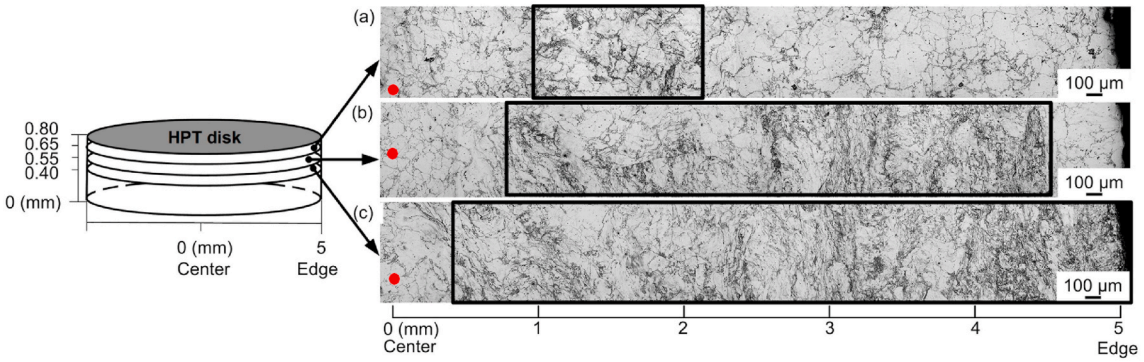

Fig. 8. Optical montages of a disc processed by HPT for 12 turns under 6.0 GPa taken at different positions of (a) 0.65, (b) 0.55 and (c) 0.40 mm from the lower surface cut parallel to the upper and lower surfaces: the severely deformed regions are contained within the rectangles denoted by solid lines on the right; the geometric centre of the disc on each image is marked with a red dot. (For interpretation of the references to colour in this figure legend, the reader is referred to the Web version of this article.)

distribution across the disk radius at the distance from the disk top surface of ~0.4 mm as shown in Fig. 7(c).

4. Discussion

This investigation provides detailed results on the microstructure and the microhardness values in the magnesium AZ80 alloy after processing by HPT for up to 12 turns. There are two major conclusions from this research.

First, the behaviour of the AZ80 alloy does not match earlier data for pure aluminium where excellent homogeneity was achieved throughout a series of HPT discs both on sectional planes cut parallel to the upper and lower surfaces [10] and on through-thickness cross-sectional planes derived by vertical sectioning [13]. Instead, the present results confirm earlier reports of heterogeneities on the through-thickness planes of various magnesium alloys after processing by HPT [12,14,15]. This difference in behaviour arises because of the limited slip systems in h.c.p. metals and the presence of long shear bands which are a common feature of magnesium alloys processed by HPT [14,15]. Thus, these shear bands tend to concentrate the deformation in highly localized areas and thereby effectively reduce the overall amounts of deformation occurring in other areas of the material. An additional microstructural feature of the AZ80 alloy is the presence of deformation twins, as shown in Fig. 5(b). The formation of deformation twins is a direct confirmation of stress localization away from the disk centre after HPT. In practice, twin boundary formation is critical for grain refinement of Mg where the interaction between twinning and dislocation glide leads to the subdivision of grains as reported earlier for a ZK60 magnesium alloy after HPT for 1/4 turn [51] and a WE43 magnesium alloy processed by HPT for 5 turns [52]. It is worth noting that the initial microstructure before HPT may influence the formation of deformation twinning. For example, ageing prior to HPT increases the fraction of low-angle grain boundaries and decreases the total fraction of deformation twin boundaries in a Mg–Dy–Al–Zn–Zr alloy where the $<\bar{2}110>$ twin boundaries have a twinning rotation angle of 86.2° [53].

Second, as reported with some other materials processed by HPT, there is clear evidence for the development of unique flow patterns after HPT processing showing well-defined swirls and vortices. This behaviour is similar in appearance to the Kelvin-Helmholtz (KH) shear instabilities which are an established and well-known effect in fluid flow. The similarities between the flow patterns in HPT processing and fluid flow was first expressed in early experiments on a duplex stainless steel [45] which specifically drew attention to the KH phenomenon [54,55]. These KH instabilities arise from the local blocking of shear deformation and they are widely known not only in fluid flow [56] but also in many other areas of physics such as plasma physics [57], atmospheric physics [58] and oceanography [59]. Generally, it was recognized that the microstructural features in the plastic deformation of metals were directly analogous to the features observed in fluid flow [60] and it was suggested that the local blocking of shear produced a rotation of obstacles leading to the formation of vortices when the imposed shear strains were sufficiently large [61]. In the present investigation, shear blocking in the AZ80 alloy may occur relatively easily through the development of representative obstacles such as twin boundaries and shear bands. There are now numerous reports providing a comprehensive summary of the formations of vortices and ordered patterns in shear deformation [62–68] and the present results are consistent with these studies on other materials when shearing is blocked during the flow process. Finally, it is important to note also that there is evidence that the shearing patterns may be influenced, and specifically shear vortices may be introduced in HPT processing, when the two HPT anvils are not in perfect alignment [69,70].

5. Summary and conclusions

1. A magnesium AZ80 alloy was processed by HPT at room temperature under a pressure of 6.0 GPa for 1/2, 1 and 12 turns. This processing led to an increased hardness from Hv ≈ 60 to Hv ≈ 140 and to significant grain refinement from ~250 μm to ~200 nm at the disc edge after 12 turns.
2. The variations in the microstructure were examined on planes parallel to the upper and lower surfaces after processing through 12 turns and on cross-sectional planes after 1/2, 1 and 12 turns. The results demonstrate the presence of significant structural heterogeneities on these planes including the presence of shear bands and twin boundaries.
3. Because of the limited slip systems in h.c.p. metals and the presence of long shear bands and twin boundaries, there is a local blocking of shear which produces well-defined vortices at high imposed strains and these vortices have similarities to the conventional Kelvin-Helmholtz shear instabilities in fluid flow.

Data availability

The raw/processed data required to reproduce these findings cannot be shared at this time as the data also forms part of an ongoing study.

CRediT authorship contribution statement

Nian Xian Zhang: Investigation, Data curation, Formal analysis, Writing - original draft. **Megumi Kawasaki:** Investigation, Writing and editing. **Hua Ding:** Data curation, Formal analysis, Supervision, Writing - original draft. **Terence G. Langdon:** Supervision, Writing - review & editing, final text.

Declaration of competing interest

The authors declare that they have no known competing financial interests or personal relationships that could have appeared to influence the work reported in this paper.

Acknowledgements

This work was supported in part by the European Research Council under ERC Grant Agreement No. 267464-SPDMETALS (TGL and NXZ) and in part by the National Science Foundation of the United States under grant no. DMR-1810343 (MK).

References

[1] R.Z. Valiev, Y. Estrin, Z. Horita, T.G. Langdon, M.J. Zehetbauer, Y.T. Zhu, Fundamentals of superior properties in bulk NanoSPD materials, Mater Res Lett 4 (2016) 1–21.
[2] T.G. Langdon, Twenty-five years of ultrafine-grained materials: achieving exceptional properties through grain refinement, Acta Mater. 61 (2013) 7035–7059.
[3] R.Z. Valiev, T.G. Langdon, Principles of equal-channel angular pressing as a processing tool for grain refinement, Prog. Mater. Sci. 51 (2006) 881–981.
[4] A.P. Zhilyaev, T.G. Langdon, Using high-pressure torsion for metal processing: fundamentals and applications, Prog. Mater. Sci. 53 (2008) 893–979.
[5] A.P. Zhilyaev, B.K. Kim, G.V. Nurislamova, M.D. Báro, J.A. Szpunar, T.G. Langdon, Orientation imaging microscopy of ultrafine-grained nickel, Scripta Mater. 46 (2002) 575–580.
[6] A.P. Zhilyaev, G.V. Nurislamova, B.K. Kim, M.D. Baró, J.A. Szpunar, T.G. Langdon, Experimental parameters influencing grain refinement and microstructural evolution during high-pressure torsion, Acta Mater. 51 (2003) 753–765.
[7] J. Wongsa-Ngam, M. Kawasaki, T.G. Langdon, A comparison of microstructures and mechanical properties in a Cu–Zr alloy processed using different SPD techniques, J. Mater. Sci. 48 (2013) 4653–4660.
[8] R.Z. Valiev, Yu.V. Ivanisenko, E.F. Rauch, B. Baudelet, Structure and deformation behaviour of Armco iron subjected to severe plastic deformation, Acta Mater. 44 (1996) 4705–4712.
[9] A. Vorhauer, R. Pippan, On the homogeneity of deformation by high pressure torsion, Scripta Mater. 51 (2004) 921–925.
[10] M. Kawasaki, R.B. Figueiredo, T.G. Langdon, An investigation of hardness homogeneity throughout discs processed by high-pressure torsion, Acta Mater. 59 (2011) 308–316.
[11] Y. Estrin, A. Molotnikov, C.H.J. Davies, R. Lapovok, Strain gradient plasticity modelling of high-pressure torsion, J. Mech. Phys. Solid. 56 (2008) 1186–1202.
[12] R.B. Figueiredo, M.T.P. Aguilar, P.R. Cetlin, T.G. Langdon, Deformation heterogeneity on the cross-sectional planes of a magnesium alloy processed by high-pressure torsion, Metall. Mater. Trans. A 42A (2011) 3013–3021.
[13] M. Kawasaki, R.B. Figueiredo, T.G. Langdon, Twenty-five years of severe plastic deformation: recent developments in evaluating the degree of homogeneity through the thickness of discs processed by high-pressure torsion, J. Mater. Sci. 47 (2012) 7719–7725.
[14] R.B. Figueiredo, T.G. Langdon, Development of structural heterogeneities in a magnesium alloy processed by high-pressure torsion, Mater. Sci. Eng. A 528 (2011) 4500–4506.
[15] A. Al-Zubaydi, R.B. Figueiredo, Y. Huang, T.G. Langdon, Structural and hardness inhomogeneities in Mg–Al–Zn alloys processed by high-pressure torsion, J. Mater. Sci. 48 (2013) 4661–4670.
[16] H.-J. Lee, S.K. Lee, K.H. Jung, G.A. Lee, B. Ahn, M. Kawasaki, T.G. Langdon, Evolution in hardness and texture of a ZK60A magnesium alloy processed by high-pressure torsion, Mater. Sci. Eng. A 630 (2015) 90–98.
[17] M. Kawasaki, Different models of hardness evolution in ultrafine-grained materials processed by high-pressure torsion, J. Mater. Sci. 49 (2013) 18–34.
[18] Y. Lou, L. Li, J. Zhou, L. Na, Deformation behavior of Mg–8Al magnesium alloy compressed at medium and high temperatures, Mater. Char. 62 (2011) 346–353.
[19] J. Kim, K. Okayasu, H. Fukutomi, Deformation behavior and texture formation in AZ80 magnesium alloy during uniaxial compression deformation at high temperatures, Mater. Trans. 54 (2013) 192–198.
[20] T.S. Pereira, C.W. Chung, R. Ding, Y.L. Chiu, Effect of equal channel angular pressing on the strength and ductility of an AZ80 alloy, IOP Conf. Ser. Mater. Sci. Eng. 4 (2009), 012022.
[21] N.X. Zhang, H. Ding, J.Z. Li, X.L. Wu, Y.L. Li, K. Xia, Microstructure and mechanical properties of ultra-fine grain AZ80 alloy processed by back pressure equal channel angular pressing, Mater. Sci. Forum 667–669 (2010) 547–552.
[22] X. Li, P. Yang, J. Li, H. Ding, Precipitation behavior, texture and mechanical properties of AZ80 magnesium alloy produced by equal channel angular extrusion, Chin. J. Mater. Res. 24 (2010) 1–9.
[23] P. Yang, L.N. Wang, Q.G. Xie, J.Z. Li, H. Ding, L.L. Lu, Influence of deformation on precipitation in AZ80 magnesium alloy, Intl J Min Metall Mater 18 (2011) 338–341.
[24] D.L. Yin, L.K. Wang, J.Q. Liu, J.T. Wang, Investigation of microstructure and strength of AZ80 magnesium alloy by ECAP and aging treatment, Kovove Mater. 49 (2011) 37–42.
[25] R. Yuan, Z. Wu, H. Cai, L. Zhao, X. Zhang, Effects of extrusion parameters on tensile properties of magnesium alloy tubes fabricated via hydrostatic extrusion integrated with circular ECAP, Mater. Des. 101 (2016) 131–136.
[26] P. Palai, N. Prabhu, B.P. Kashyap, Effect of solid die equi-channel pressing angle on β-$Mg_{17}Al_{12}$ phase morphology and mechanical behavior of AZ80 Mg alloy, J. Mater. Eng. Perform. 26 (2017) 1825–1829.
[27] G.M. Naik, G.D. Gote, S. Narendranath, Microstructural and hardness evolution of AZ80 alloy after ECAP and post-ECAP processes, Mater. Today: Proc. 5 (2018) 17763–17768.
[28] M. Avvari, S. Narendranath, Effect of secondary $Mg_{17}Al_{12}$ phase on AZ80 alloy processed by equal channel angular pressing (ECAP), Silicon India 10 (2018) 39–47.
[29] G.M. Naik, G.D. Gote, S. Narendranath, S.S. Satheesh Kumar, Microstructure and corrosion behavior of wrought AZ80 Mg alloys after the combined processes of ECAP and hot rolling, IOP Conf. Ser. Mater. Sci. Eng. A 577 (2019), 012110.
[30] D. Arpacay, S.B. Yi, M. Janeček, A. Bakkaloglu, L. Wagner, Microstructure evolution during high pressure torsion of AZ80 magnesium alloy, Mater. Sci. Forum 584–586 (2008) 300–305.
[31] S.A. Alsubaie, P. Bazarnik, M. Lewandowska, Y. Huang, T.G. Langdon, Evolution of microstructure and hardness in an AZ80 magnesium alloy processed by high-pressure torsion, J Mater Res Tech 5 (2016) 152–158.
[32] S.A. Alsubaie, Y. Huang, T.G. Langdon, Hardness evolution of AZ80 magnesium alloy processed by HPT at different temperatures, J Mater Res Tech 6 (2017) 378–384.
[33] R.B. Figueiredo, P.R. Cetlin, T.G. Langdon, Using finite element modeling to examine the flow processes in quasi-constrained high-pressure torsion, Mater. Sci. Eng. A 528 (2011) 8198–8204.
[34] R.B. Figueiredo, P.H.R. Pereira, M.T.P. Aguilar, P.R. Cetlin, T.G. Langdon, Using finite element modeling to examine the temperature distribution in quasi-constrained high-pressure torsion, Acta Mater. 60 (2012) 3190–3198.
[35] A.P. Zhilyaev, K. Oh-ishi, T.G. Langdon, T.R. McNelley, Microstructural evolution in commercial purity aluminum during high-pressure torsion, Mater. Sci. Eng. A 410–411 (2005) 277–280.
[36] K. Edalati, Z. Horita, Universal plot for hardness variation in pure metals processed by high-pressure torsion, Mater. Trans. 51 (2010) 1051–1054.
[37] J. Wongsa-Ngam, M. Kawasaki, T.G. Langdon, Achieving homogeneity in a Cu-Zr alloy processed by high-pressure torsion, J. Mater. Sci. 47 (2012) 7782–7788.
[38] S. Sabbaghianrad, M. Kawasaki, T.G. Langdon, Microstructural evolution and the mechanical properties of an aluminum alloy processed by high-pressure torsion, J. Mater. Sci. 47 (2012) 7789–7795.
[39] C. Xu, Z. Horita, T.G. Langdon, The evolution of homogeneity in processing by high-pressure torsion, Acta Mater. 55 (2007) 203–212.
[40] C. Xu, Z. Horita, T.G. Langdon, The evolution of homogeneity in an aluminum alloy processed using high-pressure torsion, Acta Mater. 56 (2008) 5168–5176.
[41] J.K. Han, K.D. Liss, T.G. Langdon, M. Kawasaki, Synthesis of a bulk nanostructured metastable Al alloy with extreme supersaturation of Mg, Sci. Rep. 9 (2019) 17186.
[42] J.K. Han, K.D. Liss, T.G. Langdon, J.I. Jang, M. Kawasaki, Mechanical properties and structural stability of a bulk nanostructured metastable aluminum-magnesium system, Mater. Sci. Eng. A 796 (2020) 140050.
[43] X.H. An, Q.Y. Lin, S.D. Wu, Z.F. Zhang, R.B. Figueiredo, N. Gao, T.G. Langdon, Significance of stacking fault energy on microstructural evolution in Cu and Cu–Al alloys processed by high-pressure torsion, Phil. Mag. 91 (2011) 3307–3326.
[44] Y. Cao, Y.B. Wang, S.N. Alhajeri, X.Z. Liao, W.L. Zheng, S.P. Ringer, T.G. Langdon, Y.T. Zhu, A visualization of shear strain in processing by high-pressure torsion, J. Mater. Sci. 45 (2010) 765–770.
[45] Y. Cao, M. Kawasaki, Y.B. Wang, S.N. Alhajeri, X.Z. Liao, W.L. Zheng, S.P. Ringer, Y.T. Zhu, T.G. Langdon, Unusual macroscopic shearing patterns observed in metals processed by high-pressure torsion, J. Mater. Sci. 45 (2010) 4545–4553.
[46] Y. Cao, Y.B. Wang, R.B. Figueiredo, L. Chang, X.Z. Liao, M. Kawasaki, W.L. Zheng, S.P. Ringer, T.G. Langdon, Y.T. Zhu, Three-dimensional shear-strain patterns induced by high-pressure torsion and their impact on hardness evolution, Acta Mater. 59 (2011) 3903–3914.
[47] W. Jiang, H. Zhou, Y. Cao, J. Nie, Y. Li, Y. Zhao, M. Kawasaki, T.G. Langdon, Y. Zhu, On the heterogeneity of local shear strain induced by high-pressure torsion, Adv. Eng. Mater. 22 (2020) 1900477.
[48] Y.Z. Tian, X.H. An, S.D. Wu, Z.F. Zhang, R.B. Figueiredo, N. Gao, T.G. Langdon, Direct observations of microstructural evolution in a two-phase Cu–Ag alloy processed by high-pressure torsion, Scripta Mater. 63 (2010) 65–68.
[49] M.H. Yoo, Slip, twinning, and fracture in hexagonal close-packed metals, Metall Trans A 12 (1981) 409–418.
[50] M.H. Yoo, J.K. Lee, Deformation twinning in hcp metals and alloys, Philos. Mag. A 63 (1991) 987–1000.
[51] S.A. Torbati-Sarraf, T.G. Langdon, Properties of a ZK60 magnesium alloy processed by high-pressure torsion, J. Alloys Compd. 613 (2014) 357–363.
[52] D.X. Liu, X. Pang, D.L. Li, C.G. Guo, J. Wongsa-Ngam, T.G. Langdon, M.A. Meyers, Microstructural evolution and properties of a hot extruded and HPT-processed resorbable magnesium WE43 alloy, Adv. Eng. Mater. 19 (2017), 1600698.
[53] R. Kocich, L. Kunčická, P. Král, T.C. Lowe, Texture, deformation twinning and hardening in a newly developed Mg–Dy–Al–Zn–Zr alloy processed with high pressure torsion, Mater. Des. 90 (2016) 1092–1099.
[54] W. Thomson, XLVI. Hydrokinetic solutions and observations, Phil Mag J Sci 42 (1871) 362–377.
[55] H. von Helmholtz, XLIII. On discontinuous movements of fluids, Phil Mag J Sci 36 (1868) 337–346.
[56] R.H. Rangel, W.A. Sirignano, Nonlinear growth of Kelvin–Helmholtz instability: effect of surface tension and density ratio, Phys. Fluids 31 (1988) 1845–1855.

[57] T.K.M. Nakamura, M. Fujimoto, Magnetic effects on the coalescence of Kelvin-Helmholtz vortices, Phys. Rev. Lett. 101 (2008) 165002.
[58] I.P.D. De Silva, H.J.S. Fernando, F. Eaton, D. Hebert, Evolution of Kelvin-Helmholtz billows in nature and laboratory, Earth Planet Sci. Lett. 143 (1996) 217–231.
[59] H. van Haren, L. Gostiaux, A deep-ocean Kelvin-Helmholtz billow train, Geophys. Res. Lett. 37 (2010) L03605.
[60] D.A. Rigney, S. Karthikeyan, The evolution of tribomaterial during sliding: a brief introduction, Tribol. Lett. 39 (2010) 3–7.
[61] R. Kulagin, Y. Beygelzimer, Y. Ivanisenko, A. Mazilkin, H. Hahn, High pressure torsion: from laminar flow to turbulence, IOP Conf. Ser. Mater. Sci. Eng. 194 (2017), 012045.
[62] Y. Beygelzimer, Vortices and mixing in metals during severe plastic deformation, Mater. Sci. Forum 683 (2011) 213–224.
[63] N.K. Sundaram, Y. Guo, S. Chandrasekar, Mesoscale folding, instability, and disruption of laminar flow in metal surfaces, Phys. Rev. Lett. 109 (2012) 106001.
[64] N. Beckmann, P.A. Romero, D. Linsler, M. Dienweibel, U. Stolz, M. Moseler, P. Gumbsch, Origins of folding instabilities on polycrystalline metal surfaces, Phys Rev Appl 2 (2014), 064004.
[65] M. Pouryazdan, B.J.P. Kaus, A. Rack, A. Ershov, H. Hahn, Mixing instabilities during shearing of metals, Nat. Commun. 18 (2017) 1611.
[66] R. Kulagin, Y. Beygelzimer, Yu. Ivanisenko, A. Mazilkin, B. Straumal, H. Hahn, Instabilities of interfaces between dissimilar metals induced by high pressure torsion, Mater. Lett. 222 (2018) 172–175.
[67] R. Kulagin, Y. Beygelzimer, A. Bachmaier, R. Pippan, Y. Estrin, Benefits of pattern formation by severe plastic deformation, Appl Mater Today 15 (2019) 236–241.
[68] A. Gola, R. Schwaiger, P. Gumbsch, L. Pastewka, Pattern formation during deformation of metallic nanolaminates, Phys Rev Mater 4 (2020), 013603.
[69] Y. Huang, M. Kawasaki, T.G. Langdon, Influence of anvil alignment on shearing patterns in high-pressure torsion, Adv. Eng. Mater. 15 (2013) 747–755.
[70] Y. Huang, M. Kawasaki, T.G. Langdon, An investigation of flow patterns and hardness distributions using different anvil alignments in high-pressure torsion, J. Mater. Sci. 48 (2013) 4533–4542.